Effect of Zr Content on Formation and Optical Properties of the Layered $PbZr_xTi_{1-x}O_3$ Films *

Yang-Yang Xu(许阳阳)[1,2], Yu Wang(王宇)[1,2], Ai-Yun Liu(刘爱云)[1], Wang-Zhou Shi(石旺舟)[1], Gu-Jin Hu(胡古今)[1**], Shi-Min Li(李世民)[2], Hui-Yong Deng(邓惠勇)[2], Ning Dai(戴宁)[2**]

[1]*Department of Physics, College of Mathematics and Science, Shanghai Normal University, Shanghai 200234*
[2]*National Laboratory for Infrared Physics, Shanghai Institute of Technical Physics, Chinese Academy of Sciences, Shanghai 200083*

(Received 4 November 2019)

$PbZr_xTi_{1-x}O_3$ (PZT) films are fabricated on F-doped tin oxide (FTO) substrates using chemical solutions containing PVP polymer and rapid thermal annealing processing. The dependence of the layered PZT multilayer formation and their optical properties on the Zr content x are examined. It is found that all the PZT films are crystallized and exhibit 110-preferred orientation. When x varies in the region of 0–0.8, the PZT films display lamellar structures, and a high reflection band occurs in each optical reflectance spectrum curve. Especially, those PZT films with Zr/Ti atomic ratio of 35/65–65/35 show clearly layered cross-sectional morphologies arranged alternatively by porous and dense PZT layers, and have a peak optical reflectivity of >70% and a band width of >45 nm. To obtain the optimal Bragg reflection performance of the PZT multilayers, the Zr content should be selected in the range of 0.35–0.65.

PACS: 68.55.−a, 68.37.−d, 78.66.−w, 81.05.−t, 77.55.hj DOI: 10.1088/0256-307X/37/2/026801

Ferroelectric materials have been regarded as an ideal media for building photonic devices with tunable characteristic parameters because of their high transparency in the region of visible to infrared, large refractive index, and especially their large electro-optical coefficient. For instance, the photonic band gap (PBG) of 3D inverse opal photonic crystal (PC) fabricated by Lead lanthanum zirconate titanate (PLZT) has been tuned continuously with a dc bias.[1] There would be a 2-nm change in the PBG of the 1D PC consisting of $MgO/Ba_{0.7}Sr_{0.3}TiO_3$ multilayer by applying electric filed, and there would be a 8.5 nm variation in the PBG of the PC arranged alternatively by ZnO:Al and PLZT layers under a voltage of 8 V.[2,3]

Recently, Hu *et al.* developed a simple and effective processing route to fabricate quasiperiodic ferroelectric multilayers on different supports based on one single chemical solution.[4–8] The obtained ferroelectric multilayers exhibit excellent performance as Bragg reflectors and optical microcavities. This approach exploits phase-separation and electrostatic interaction mechanisms, and can be described briefly as follows. (i) For a polycrystal ferroelectric film, those crystal grain surfaces with non in-plane electric polarization component display electric polarity. (ii) In spin-coating films, polymers with polar groups segregate from precursor solution via phase-segregation, and are simultaneously driven to polar crystal grain surfaces through electrostatic attraction, where polymers condense into nanoscale aggregations. These polymer particles distribute preferentially in the bottom of the as-deposited gel film. (iii) When the gel film is sintered at high temperature and converted into ferroelectric phase, polymer aggregations are thermally decomposed and hence have left pores in the film, giving rise to a bilayer consisting of dense and pore-imbedded ferroelectric layers. The building block in a ferroelectric multilayer is the bilayer comprising of a pair of dense and porous ferroelectric films.

The polymer and polar surfaces play a crucial role in creating ferroelectric multilayers, and significantly affect multilayers' physical states and natures. The surface electric polar strength of a ferroelectric film is determined by its crystallographic phase and ingredient. The film crystallographic quality is closely related to crystallization temperature. Shang *et al.* examined the dependence of microstructures and optical properties of $Ba_{0.9}Sr_{0.1}TiO_3$ multilayers on polymer type/content, and obtained the optimal polymer amount.[9] Zhang *et al.* explored the evolution of the microstructure, ferroelectric, dielectric and optical characteristics of $PbZr_{0.4}Ti_{0.6}O_3$ films with annealing temperature, and found that 650℃ is the best sintering temperature for constructing high performance $PbZr_{0.4}Ti_{0.6}O_3$ multilayers.[8]

It is well-known that the ferroelectricity of ferroelectrics is determined by their composition, thus it is necessary to explore the correlation between the ferroelectric multilayer formation, optical property and the ingredient.[10] The microstructures and optical reflection characteristics of the PZT films with various Zr or Ti contents are investigated systemically in this

*Supported by the Frontier Science Research Project of Chinese Academy of Sciences (No. QYZDJ-SSW-SLH018), the National Natural Science Foundation of China (Nos. 11174307 and 11933006), and the National Key Basic Research Program of China (No. 2016YFB0402405).

**Corresponding author. Email: hugj@shnu.edu.cn; ndai@mail.sitp.ac.cn

© 2020 Chinese Physical Society and IOP Publishing Ltd

work to determine the best Zr/Ti atomic molar ratio range, to achieve optimal Bragg reflection performance of $PbZr_xTi_{1-x}O_3$ (PZT) multilayers and to promote application of ferroelectric compounds in the field of PBG engineering.

We took 0.4-M/L PZT precursor solutions containing PVP synthesized by the method introduced by Takenaka and Kozuka.[11] The Zr/Ti ratio was adjusted by changing dosage of starting materials of titanium isopropoxide $Ti(OC_3H_7)_4$ and zirconium propoxide $Zr(OC_3H_7)_4$. Cleaned glass slices coated with a layer of transparent conductive FTO were used as substrates, and were pre-heat treated at 650℃ for 10 min to enhance bonding between FTO and PZT films. Spin-coating/annealing process was utilized to fabricate PZT films, and spinning rate for deposition of the PZT wet gel film was 2600 rounds per minute. In each spin-coating/annealing step (called a growing-period), the deposited wet gel film was dried at 180℃ for 5 min, then pre-fired at 380℃ for 6 min to remove residual organics, and followed by annealing at 650℃ for 8 min. This procedure was repeated 14 times to obtain desired PZT films. A series of PZT films (with $x = 0$, 0.3, 0.4, 0.5, 0.6, 0.7, and 1) were prepared, for simplicity, they were marked as samples A, B, C, D, E, F, and G, respectively.

The crystallographic quality of the grown PZT films was characterized by an x-ray diffraction meter (D8 Focus, Bruker, Karlsruhe, Germany). The cross-sectional morphologies of the specimens were observed via a field emission scanning electron microscope (SEM, S4800, Hitachi, Tokyo, Japan). The room temperature reflectance spectra of the PZT films were measured by a Perkin Elmer Lambda 800/900 UV/visible spectrometer. The incident light was almost perpendicular to the sample's surface.

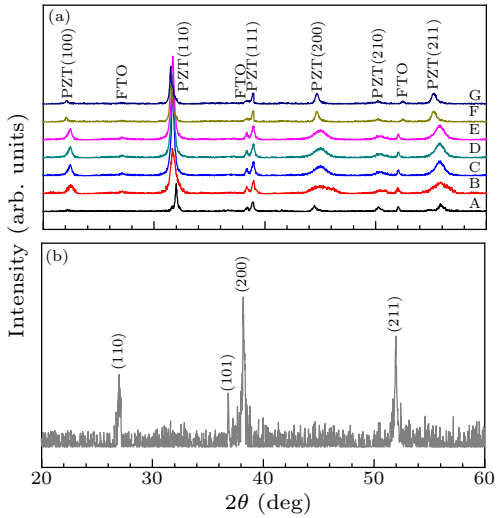

Fig. 1. X-ray diffraction patterns for (a) the PZT films and (b) the FTO substrate.

Figures 1(a) and 1(b) present the x-ray diffraction data for the PZT films with various Zr contents and the FTO buffer layer. From Fig. 1, it can be clearly seen that the x-ray diffraction patterns are dominated by the diffraction peaks of (110) crystal planes besides the weak diffraction peaks from (100) and (111) crystal planes, indicating that each PZT film has been fully crystallized and has a polycrystalline structure with a 110-preferred orientation. In addition, for those PZT films where the Zr content is unequal 0 or 1, their corresponding diffraction peak locations nearly coincide.

Figure 2 shows a panel of fractured-section morphological SEM photos of samples A, B, C, D, E, F, and G. Their film thicknesses derived from the SEM images are ∼1.90, 1.58, 1.40, 1.77, 2.00, 1.45, and 1.66 μm, respectively. There is a ∼600 nm thickness deviation between specimens C and E. It is known that in the sol-gel process the deposited gel film thickness d in a growing-period is determined by the spinning rate ω, substrate diameter D, and solution concentration C. This satisfies the equation[12]

$$d = k\omega^{-m}D^{-n}C, \tag{1}$$

where k, m, and n are constants related with natures of both solution and substrate surface. Because the used ω, D, C, and the growing-period number are identical for all PZT films, we believe that the discrepancy in film thickness originates chiefly from different solution properties and inconsistency in each artificial dropping sol operation.

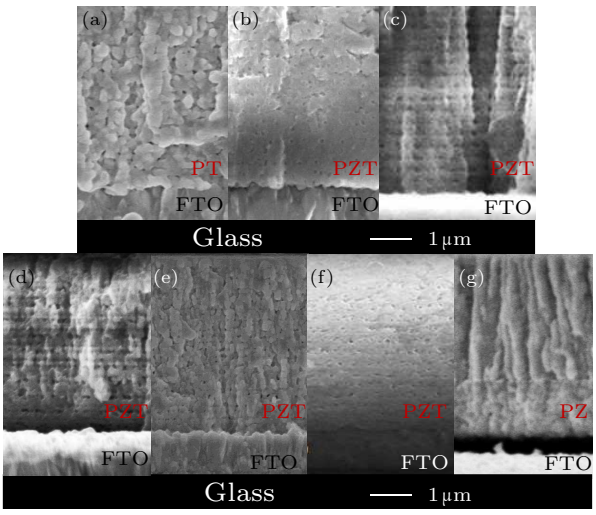

Fig. 2. Cross-sectional SEM images of samples A–G.

By carefully analyzing the SEM images, it can be observed that sample G has a relative dense cross section and there is no delamination in the direction perpendicular to film surface. However, specimens C, D, and E reveal evident and regular lamellar textures consisting of dense and porous PZT layers, similar to cross-sectional morphologies of $Ba_{0.9}Sr_{0.1}TiO_3$ and $PbZr_{0.4}Ti_{0.6}O_3$ multilayers reported in Refs. [4–8] The other three counterparts also seem to exhibit the weak

delamination phenomenon, while their regularity and distinguishability are poor in comparison to the other three PZT films.

At room temperature, PZT oxides with Zr atomic content percentages of 0.95–1 are antiferroelectric and do not exhibit spontaneous polarization.[13,14] Additionally, the surface of FTO conductive thin film also has no electric polarity. Hence, PVP polymer aggregations produced by phase-separation distribute randomly within the wet gel film, resulting in a uniform PZT film, as is the case in sample G. In contrast, specimens C, D, and E possess larger remanent polarization values due to their compositions being near or within the morphotropic phase boundary where ferroelectric tetragonal and rhombic states coexist.[6,8] Correspondingly, a large amount of polarization charges will occur on the PZT film surface and bring a strong electrostatic attraction force to PVP polymer with opposite polar groups. This is a radical reason leading to the appearance of a distinct and ordered layered structure in $PbZr_{0.4}Ti_{0.6}O_3$, $PbZr_{0.5}Ti_{0.5}O_3$, and $PbZr_{0.6}Ti_{0.4}O_3$ films. The x-ray diffraction experimental results prove this conclusion indirectly. Generally, spontaneous polarization parallel with the direction of ferroelectric crystal growth. The crystal grains growing along $\langle 100\rangle$, $\langle 110\rangle$, and $\langle 111\rangle$ directions have a component of electric polarization P_s perpendicular to the crystal surface. The surface electric polarity is stronger when P_s is larger. Compared with samples C, D, and E, specimen A, B or F renders a smaller average intensity of diffraction peaks, meaning that the PZT film surface polarity is relatively weak; i.e., only a part of polymer in the coating solution can be absorbed on the substrate surface. Consequently, the thickness of the dense PZT layer is much larger than that of the porous PZT layer.

According to thin film optical theory, when the optical thickness of each layer in a periodic stack consisting of two different media is a quarter of the central wavelength λ_0, the spectroscopic reflectivity enhances at λ_0 owing to constructive interference and a high reflectivity band centered at λ_0 appears in the reflectance spectrum curve. The peak reflectivity R and stop-band width $\Delta\lambda$ are determined by

$$R = \left[\frac{(n_H/n_L)^S - n_S/n_0}{(n_H/n_L)^S + n_S/n_0}\right]^2, \tag{2}$$

$$2\Delta\lambda = 2\lambda_0\Delta g,$$

$$\Delta g = \frac{2}{\pi}\sin^{-1}\left(\frac{n_H - n_L}{n_H + n_L}\right), \tag{3}$$

where n_H, n_L, n_S, and n_0 denote, respectively, refractive indices of the coating materials, substrate, and air, while S presents the period number. Both increase with decreasing optical phase difference between the high and the low refractive index layers at a given S.

Since effective refractive index of the compact-PZT layer is high than that of the loosened-PZT layer, one-dimensional quasiperiodic multilayer stacks as dielectric mirrors will form through regular alternating arrangement of dense and porous PZT thin films. Figure 3 plots the optical reflectivity as a function of wavelength for these PZT films at room temperature. As is expected, a narrower reflection band with a smaller average reflectivity exists in each curve for specimens A, B, and F. For sample G, the reflectance spectrum exposes its ordinary optical thin film feature only. However, samples C, D, and E display a relative broader high reflectivity band, and the corresponding central wavelengths of the reflection band/band width/peak reflectivity are 508 nm/59 nm/81%, 536 nm/58 nm/77%, and 570 nm/49 nm/71%, rendering good optical performance as dielectric Bragg reflectors. As shown in Fig. 2, the arrangement of dense and porous PZT layers in samples C, D, and E is well-ordered cross section; i.e., the optical phase mismatch between high and low refractive index layers is small, giving rise to a broader reflection band and a higher value of peak reflectivity.

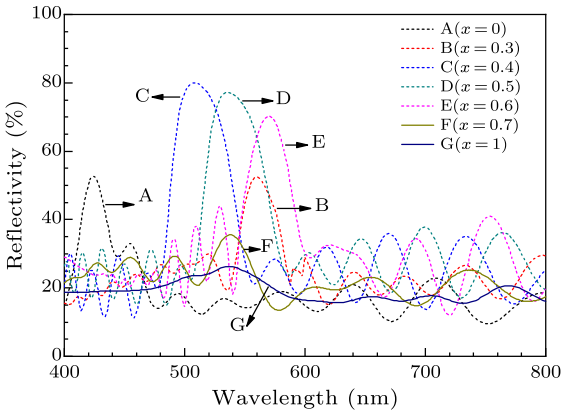

Fig. 3. Room-temperature reflectance curves of specimens A–G.

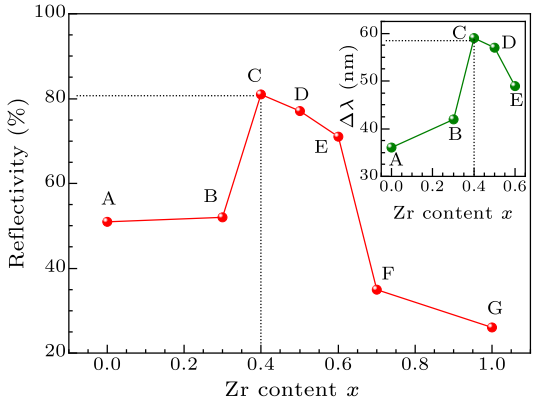

Fig. 4. Dependence of the PZT films' peak reflectivities on Zr content. The inset shows the variation of band width with Zr content.

Figure 4 represents the dependence of peak reflectivity on Zr content x, and the inset narrates the variation of the reflection band width with x. Both the

peak reflectivity and band width increase with x and we get maxima at $x = 0.4$, and then a gradual decrease with increasing x. When x is in the range of 0.35–0.65, the $PbZr_xTi_{1-x}O_3$ films exhibit peak reflectivities over 70% and reflection-band widths over 45 nm. The Bragg reflectance performance is the best for the $PbZr_{0.4}Ti_{0.6}O_3$ multilayer.

In summary, we have grown a series of PZT films on glass slices coated with transparent and conductive FTO using precursor solutions with PVP additive. It is revealed that Zr or Ti content significantly affects the formation and optical properties of the PZT multilayers. It is found that all the PZT films are well-crystallized, and reflection bands exist in the reflectance curves of the PZT films with $x < 0.9$. When x is around morphotropic phase boundary, the PZT films display well-ordered lamellar textures consisting of the dense and porous PZT layers, and exhibit peak reflectivities of over 70% and band widths of over 45 nm. To obtain the optimal Bragg optical reflection performance of PZT films, Zr content should be selected in the range 0.35–0.65.

The authors thank R. Cong, Y. Sun, X. J. Meng, Zh. M. Huang, F. Liu, and J. T. Zhang for their help in experimental measurements and valuable discussions of experimental data.

References

[1] Li B, Zhou J, Li L, Wang X J, Liu X H and Zi J 2003 *Appl. Phys. Lett.* **83** 4704
[2] Jim K L, Wang D Y, Leung C W, Choy C L and Chan H L 2008 *J. Appl. Phys.* **103** 083107
[3] Oh J M, Hoshina T, Takeda H and Tsurumi T 2013 *Appl. Phys. Express* **6** 062001
[4] Hu G J, Chen J, An D L, Chu J H and Dai N 2005 *Appl. Phys. Lett.* **86** 162905
[5] Hong X K, Hu G J, Chen J, Chu J H, Dai N and Wu H Z 2006 *Appl. Phys. Lett.* **89** 082902
[6] Hu G J, Hong X K, Chu J H and Dai N 2007 *Appl. Phys. Lett.* **90** 162904
[7] Hong X K, Hu G J, Shang J L, Bao J, Chu J H and Dai N 2007 *Appl. Phys. Lett.* **90** 251911
[8] Zhang T, Hu G J, Bu H J, Wu J, Chu J H and Dai N 2010 *J. Appl. Phys.* **107** 084103
[9] Shang J L, Hu G J, Zhang T, Sun Y, Wu J, Chu J H and Dai N 2009*J. Am. Ceram. Soc.* **92** 539
[10] Gong S, Wang Y H, Zhao X Y, Zhang M, Zhao N and Duan Y F 2011 *Chin. Phys. Lett.* **28** 087402
[11] Takenaka S and Kozuka H 2001 *Appl. Phys. Lett.* **79** 3485
[12] Macleod H A 1986 *Thin-Film Optical Filters* 2nd edn (New York: Macmillan Press) p 412
[13] Shirane G, Sawaguchi E and Takagi Y 1951 *Phys. Rev.* **84** 476
[14] Hu C S, Sun X, Luo Z L and Gao C 2014 *Chin. Phys. Lett.* **31** 110501